The Plant Cell, Vol. 15, 1227–1241, May 2003, www.plantcell.org © 2003 American Society of Plant Biologists

(*E*)-β-Ocimene and Myrcene Synthase Genes of Floral Scent Biosynthesis in Snapdragon: Function and Expression of Three Terpene Synthase Genes of a New Terpene Synthase Subfamily

Natalia Dudareva,[a,1,2] Diane Martin,[b] Christine M. Kish,[a] Natalia Kolosova,[a,3] Nina Gorenstein,[a] Jenny Fäldt,[b] Barbara Miller,[b] and Jörg Bohlmann[b,2]

[a] Department of Horticulture and Landscape Architecture, Purdue University, West Lafayette, Indiana 47907
[b] Biotechnology Laboratory and Departments of Botany and Forest Sciences, University of British Columbia, Vancouver, British Columbia, Canada V6T 1Z3

Snapdragon flowers emit two monoterpene olefins, myrcene and (*E*)-β-ocimene, derived from geranyl diphosphate, in addition to a major phenylpropanoid floral scent component, methylbenzoate. Emission of these monoterpenes is regulated developmentally and follows diurnal rhythms controlled by a circadian clock. Using a functional genomics approach, we have isolated and characterized three closely related cDNAs from a snapdragon petal-specific library that encode two myrcene synthases (*ama1e20* and *ama0c15*) and an (*E*)-β-ocimene synthase (*ama0a23*). Although the two myrcene synthases are almost identical (98%), except for the N-terminal 13 amino acids, and are catalytically active, yielding a single monoterpene product, myrcene, only *ama0c15* is expressed at a high level in flowers and contributes to floral myrcene emission. (*E*)-β-Ocimene synthase is highly similar to snapdragon myrcene synthases (92% amino acid identity) and produces predominantly (*E*)-β-ocimene (97% of total monoterpene olefin product) with small amounts of (*Z*)-β-ocimene and myrcene. These newly isolated snapdragon monoterpene synthases, together with Arabidopsis AtTPS14 (At1g61680), define a new subfamily of the terpene synthase (TPS) family designated the *Tps-g* group. Members of this new *Tps-g* group lack the RRx_8W motif, which is a characteristic feature of the *Tps-d* and *Tps-b* monoterpene synthases, suggesting that the reaction mechanism of *Tps-g* monoterpene synthase product formation does not proceed via an RR-dependent isomerization of geranyl diphosphate to *3S*-linalyl diphosphate, as shown previously for limonene cyclase. Analyses of tissue-specific, developmental, and rhythmic expression of these monoterpene synthase genes in snapdragon flowers revealed coordinated regulation of phenylpropanoid and isoprenoid scent production.

INTRODUCTION

Monoterpenes, the C_{10} members of the terpenoid family of natural products, are common constituents of floral scents that function as volatile cues to attract insects or other pollinators (Knudsen et al., 1993; Dobson, 1994; Dudareva and Pichersky, 2000). These floral odors may have evolved from protective functions of monoterpenes in vegetative and reproductive organs of angiosperms and gymnosperms (Bohlmann et al., 2000a). At present, information about monoterpene biosynthesis and their regulation comes mostly from studies with vegetative tissues, in which they serve as compounds in direct and indirect defense against herbivores and as protection against pathogens. A large group of terpene synthase (TPS) genes and enzymes has been characterized in vegetative tissues of several angiosperms and gymnosperms (Bohlmann et al., 1998; Davis and Croteau, 2000; Aubourg et al., 2002). However, to date, only two terpene synthase genes of floral scent biosynthesis have been reported. Linalool synthase, a monoterpene synthase that catalyzes the formation of an acyclic monoterpene alcohol, linalool, was the first to be isolated and characterized in *Clarkia breweri* flowers (Pichersky et al., 1995; Dudareva et al., 1996), and a sesquiterpene synthase gene for the formation of germacrene D was characterized recently in *Rosa hybrida* petals (Guterman et al., 2002).

Several features of snapdragon flowers involved in the attraction of bee pollinators, such as the composite floral scent of phenylpropanoids and isoprenoids, the concentration of scent production and emission in the lobes of a zygomorphic flower, and the rhythmic nature of emission, make it a very attractive system in which to decipher the biochemical and molecular genetic regulation of floral scent biology (Dudareva et al., 2000; Kolosova et al., 2001a, 2001b). The major components in the fragrance of snapdragon flowers (cv Maryland True Pink) are the aromatic ester methylbenzoate, which is derived from the phenylpropanoid pathway (~60% of total floral scent output), and two monoterpene olefins, myrcene and (*E*)-β-ocimene (~8 and 20% of total floral scent output, respectively), both of which are derived from geranyl diphosphate (Dudareva et al., 2000). Investigation of the regulation of methylbenzoate emission showed that the major factors controlling its production

[1] To whom correspondence should be addressed. E-mail dudareva@hort.purdue.edu; fax 1-765-494-0391.
[2] These authors contributed equally to this work.
[3] Current address: Biotechnology Laboratory, University of British Columbia, Vancouver, BC, Canada V6T 1Z3.
Article, publication date, and citation information can be found at www.plantcell.org/cgi/doi/10.1105/tpc.011015.

and emission during flower development include the regulation of expression of the benzoic acid carboxyl methyltransferase (BAMT) gene, which encodes the final enzyme in methylbenzoate biosynthesis, and the level of supplied substrate (benzoic acid) for the reaction (Dudareva et al., 2000). Moreover, it was shown that the level of substrate also plays a major role in the regulation of the circadian emission of methylbenzoate in diurnally (snapdragon) and nocturnally (petunia cv Mitchell and *Nicotiana suaveolens*) emitting flowers (Kolosova et al., 2001a). In contrast to recent progress in our understanding of the regulation of methylbenzoate formation and emission in snapdragon flowers (Dudareva et al., 2000; Kolosova et al., 2001a, 2001b), very little is known about the enzymes and genes responsible for the biosynthesis of floral monoterpenes and the molecular mechanisms that control the pathway flux to these volatile compounds.

Here, we present a detailed analysis of the production of the volatile monoterpenes myrcene and (*E*)-β-ocimene in snapdragon flowers. Developmental and rhythmic emission of these monoterpene compounds was determined, as was emission in the absence of environmental cues (in continuous dark and continuous light), to evaluate if a circadian, endogenous clock controls their emission rhythmicity. Because many monoterpene synthases catalyze the formation of multiple products (Bohlmann et al., 1998; Wise and Croteau, 1999; Davis and Croteau, 2000), we also analyzed whether myrcene and ocimene biosynthesis requires specialized monoterpene synthases for each component or if a multifunctional synthase similar to myrcene/(*E*)-β-ocimene synthase from Arabidopsis (Bohlmann et al., 2000b) is involved. Three monoterpene synthases have been isolated from snapdragon flowers using a functional genomics approach, and biochemical characterization of the enzymes encoded by these three cDNAs showed that they represent two myrcene synthases and an (*E*)-β-ocimene synthase, enzymes responsible for the biosynthesis of two major monoterpene compounds of snapdragon floral scent. Analyses of the tissue-specific, developmental, and rhythmic expression of monoterpene synthase genes revealed coordinated regulation of phenylpropanoid and isoprenoid scent production in snapdragon flowers.

RESULTS

Developmental and Rhythmic Emission of Myrcene and (*E*)-β-Ocimene from Snapdragon Flowers

We showed previously that snapdragon floral scent is dominated by (*E*)-β-ocimene, myrcene, and methylbenzoate (Dudareva et al., 2000). To determine variations in the emission of myrcene and (*E*)-β-ocimene during flower development, we performed time-course headspace collections from single, living flowers at 24-h intervals followed by gas chromatography–mass spectrometry (GC-MS) analysis. Headspace collections began with mature flower buds at 1 day before opening and ended 12 days later. Unopened flowers (buds) and 1-day-old flowers released little, if any, detectable myrcene and (*E*)-β-ocimene (Figure 1A). Monoterpene emission increased strongly on the second day after anthesis [50 and 39% of the maximum peak levels for myrcene and (*E*)-β-ocimene, respectively]. Emission of myrcene peaked on days 5 to 7 and remained relatively high for the next 2 to 3 days, whereas emission of (*E*)-β-ocimene peaked sharply on days 6 to 7 and declined gradually thereafter. Although the emission of (*E*)-β-ocimene by snapdragon flowers was four times higher than that of myrcene, with maximum levels at 31.9 and 8.3 μg per flower per 24 h on day 6 after anthesis, respectively, there was no difference in the emission of these monoterpenes in old (11- and 12-day-old) flowers (Figure 1A).

To determine diurnal fluctuations in the emission of myrcene and (*E*)-β-ocimene in snapdragon flowers, floral volatile compounds were collected from 3-day-old flowers at seven time points over a period of 48 h of two normal light/dark cycles (12 h of light/12 h of dark). This experiment revealed that, as with methylbenzoate (Kolosova et al., 2001a), emission of the two monoterpenes follows diurnal cycles, with the highest emission rate between 11 AM and 6 PM (Figure 1B). To determine whether this diurnal rhythmicity of myrcene and (*E*)-β-ocimene emission is controlled by irradiation level or by a circadian clock, plants were grown in a 12-h-light/12-h-dark period at a constant temperature of 25°C and then transferred to conditions of either continuous light or continuous dark. Floral volatiles were collected at seven time points during each 24-h interval for 120 h (5 days) (Figures 2A and 2B). Flowers used for headspace analysis were 3 days old at the beginning of the time-course experiment. Results obtained show that the rhythmic emission of monoterpene compounds displayed a "free-running" cycle in the absence of environmental cues (in continuous dark or continuous light), indicating the circadian nature of diurnal rhythmicity (Figure 2).

Cloning and Sequence Characterization of Snapdragon Monoterpene Synthases

Formation of the two major monoterpene floral scent components, myrcene and (*E*)-β-ocimene, could involve specialized monoterpene synthases for each of the two compounds or a multifunctional synthase. As part of an ongoing effort to isolate genes involved in floral scent production in snapdragon flowers, we randomly sequenced 792 clones (ESTs) from a cDNA library constructed from mRNA isolated from petals (upper and lower lobes) of 1- to 5-day-old flowers, the parts of the flower highly specialized for floral scent biosynthesis (Dudareva et al., 2000). A search of this EST database for potential monoterpene synthases revealed three unique cDNA clones (designated *ama0c15*, *ama0a23*, and *ama1e20*) with overall high sequence similarity (Figure 3) to angiosperm monoterpene synthases of the *Tps-b* cluster of the *TPS* gene family of higher plants (Bohlmann et al., 1998; Aubourg et al., 2002) as well as with linalool synthase from *Clarkia* (Dudareva et al., 1996) and gymnosperm monoterpene synthases of the *Tps-d* cluster (Bohlmann et al., 1999).

The *ama0c15* EST represented a full-length cDNA clone of 1901 nucleotides. This clone had a very short 5′ untranslated region (only 6 nucleotides) and encoded an open reading frame of 1743 nucleotides corresponding to a predicted protein of 581 amino acids with a calculated molecular weight of 66,701 and a pI of 6.04 (Figure 4). The other EST cDNA clones,

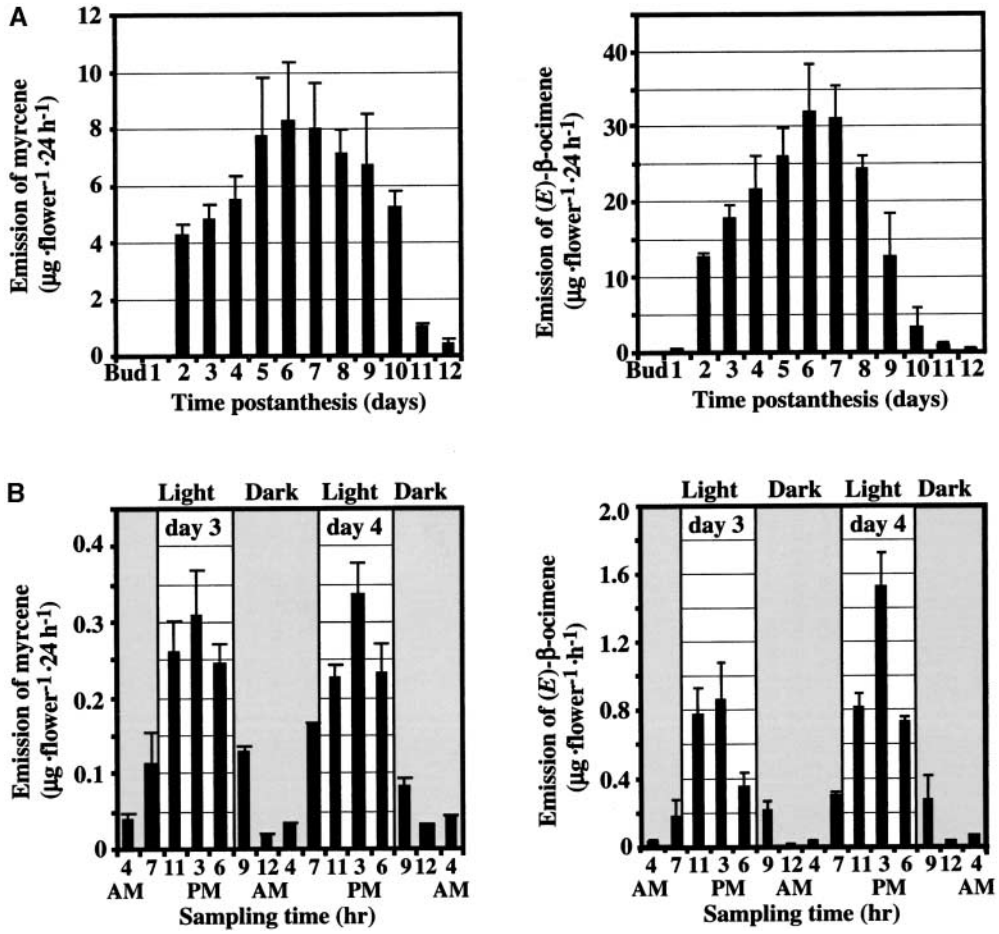

Figure 1. Myrcene and (*E*)-β-Ocimene Emission from Snapdragon Flowers.

(A) Emission of myrcene (left) and (*E*)-β-ocimene (right) during the life span of the flower, from mature flower buds 1 day before opening to 12 days after anthesis.

(B) Rhythmic emission of myrcene (left) and (*E*)-β-ocimene (right) from 3- and 4-day-old snapdragon flowers during two normal light/dark cycles. Shaded and unshaded areas correspond to dark and light, respectively.

Each graph represents the average of three to five independent experiments. Standard deviations are indicated by vertical bars.

ama0a23 and *ama1e20*, were found to be truncated at their 5′ ends. Two methods, 5′ rapid amplification of cDNA ends (RACE) and cDNA library screening, were used to recover corresponding full-length clones for these ESTs. Initial 5′ RACE based on truncated *ama1e20* resulted in the isolation of an independent cDNA clone identical to *ama0c15*. However, screening of the cDNA library using the truncated *ama1e20* EST probe yielded a full-length cDNA clone corresponding to *ama1e20* of 2412 nucleotides, with an open reading frame of 1752 nucleotides that encoded a predicted protein of 584 amino acids (Figure 4) with a calculated molecular weight of 67,349 and a pI of 6.11. The proteins encoded by *ama0c15* and *ama1e20* were 98% identical to each other, and the differences were found only within the N-terminal 13 amino acids. In addition, the *ama0c15* protein was three amino acids shorter than *ama1e20*. The third cDNA clone, *ama0a23*, was nearly full length, with 1844 bp lacking the ATG start codon and the first codon of its open reading frame lining up with the position of codon 10 in *ama1e20*. Using 5′ RACE, a 1902-bp full-length cDNA sequence of *ama0a23* was recovered that encoded an open reading frame of 1737 nucleotides corresponding to a protein of 579 amino acids (Figure 4) with a calculated molecular weight of 66,724 and a pI of 6.15. This cDNA clone has 92% amino acid identity to *ama1e20* and *ama0c15*.

Despite overall sequence similarity to other monoterpene synthases, the deduced proteins of the snapdragon monoterpene synthase cDNAs *ama0c15*, *ama0a23*, and *ama1e20* are quite different from the known monoterpene synthases of angiosperms (*Tps-b* group; 22 to 27% amino acid identity) and gymnosperms (*Tps-d* group; 22 to 27% amino acid identity). Strikingly, the predicted snapdragon proteins do not contain the RRx_8W motif (Figure 4), which is a key feature of all mono-

terpene synthases of the *Tps-b* and *Tps-d* groups characterized to date (Bohlmann et al., 1998; Aubourg et al., 2002).

Functional Identification and Characterization of *ama0c15*, *ama0a23*, and *ama1e20*

For functional characterization of the TPS proteins encoded by *ama0c15*, *ama0a23*, and *ama1e20*, the cDNAs were subcloned into the pET-TOPO D100 expression vector, and the encoded proteins then were expressed separately in *Escherichia coli* BL21-CodonPlus(DE3). Extracts of isopropylthio-β-galactoside–induced bacteria were assayed for monoterpene synthase, sesquiterpene synthase, and diterpene synthase activities using the corresponding prenyl diphosphate substrates geranyl diphosphate (GPP), farnesyl diphosphate, and geranylgeranyl diphosphate. Enzymatic formation of terpene olefins was observed only with GPP as a substrate, not with farnesyl diphosphate or geranylgeranyl diphosphate, identifying all three genes as monoterpene synthases. No oxygenated monoterpene products were detected. Extracts prepared from *E. coli* (same strain) transformed with pET-TOPO D100 lacking a cDNA insert and heat-denatured enzyme preparations served as controls for monoterpene formation independent of snapdragon TPS. These extracts did not yield any detectable amounts of monoterpene product.

Products formed by recombinant snapdragon monoterpene synthases with GPP as a substrate were analyzed by GC-MS. The two very similar proteins encoded by *ama1e20* and *ama0c15* each yielded a single monoterpene product of the same retention time. This product was identified as myrcene based on a comparison of retention times and mass spectra with those of an authentic myrcene standard (Figure 5). Protein encoded by *ama0a23* also formed a single major product with GPP that was identified based on retention time and mass spectral data as (*E*)-β-ocimene (97% of total monoterpene olefin product), along with two minor products identified as (*Z*)-β-ocimene (2%) and myrcene (1%) (Figure 6). Together, these three monoterpene synthase genes, *ama1e20*, *ama0c15*, and *ama0a23*, account for the major monoterpene compounds of floral scent in snapdragon.

To test the presence of corresponding monoterpene synthase activities in snapdragon floral tissue, cell-free extracts were prepared from upper and lower petal lobes of 5-day-old flowers and assayed with GPP as a substrate. Cell-free extracts pro-

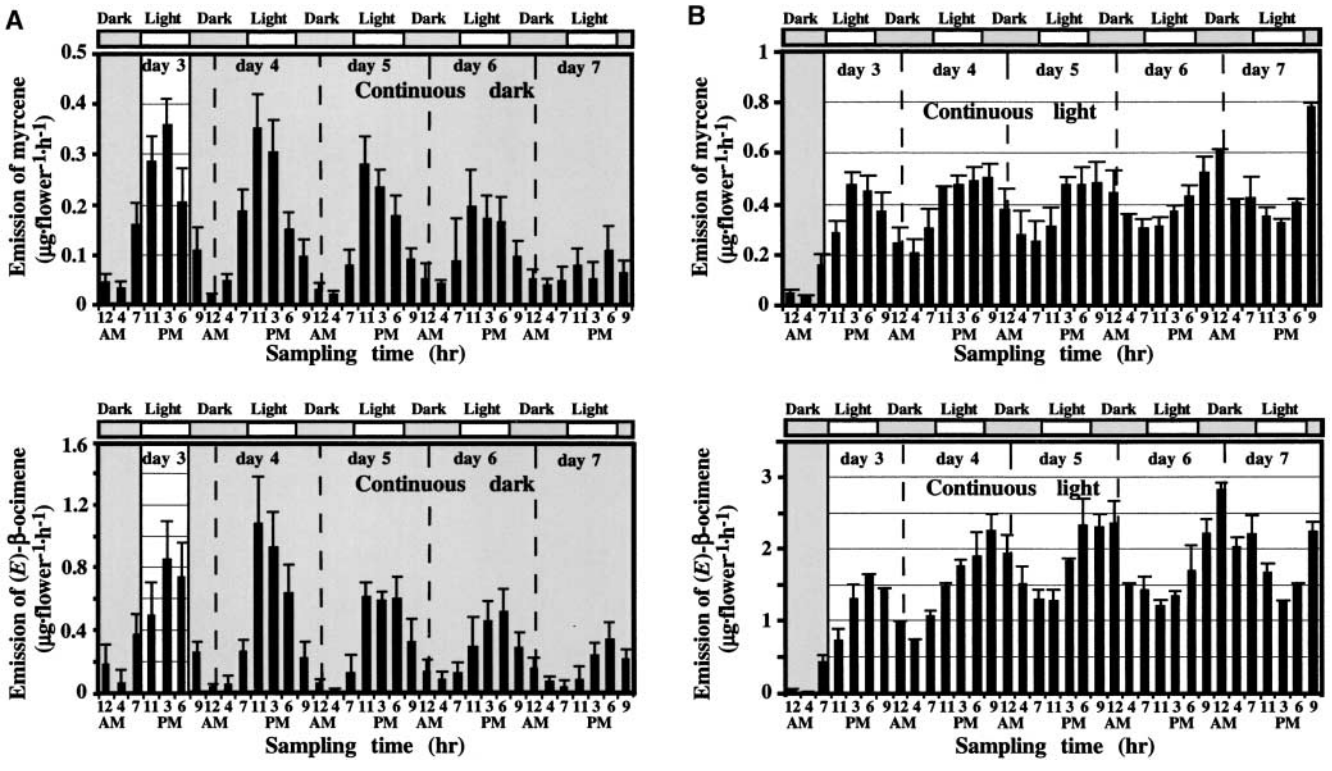

Figure 2. Emission of Myrcene and (*E*)-β-Ocimene from Snapdragon Flowers Exposed to Different Light/Dark Conditions.

(A) Intact flowers were exposed to the normal day/night cycle (12/12 h day/night) followed by continuous dark for 4 days.

(B) Intact flowers were exposed to the normal day/night cycle (12/12 h day/night) followed by continuous light (100 μmol·m^{-2}·s^{-1}) for 4 days.

Headspace collections were performed at seven time points during a 24-h interval. Shaded and unshaded areas correspond to dark and light, respectively. The corresponding theoretical light/dark cycle is indicated at the top of each graph by unshaded bars (light period) and shaded bars (dark period). Each graph represents the average of three to five independent experiments. Standard deviations are indicated by vertical bars.

	(1)	(2)	(3)	(4)	(5)	(6)	(7)	(8)	(9)	(10)	(11)	(12)	(13)	(14)	(15)	(16)	(17)	(18)	(19)	(20)	(21)
(1) *Quercus ilex* Myrcene S.	100																				
(2) *Artemisisa annua* (-)-β-Pinene S.	**44**	100																			
(3) *Arabidopsis thlaiana E*-β-Ocimene S.	**42**	**37**	100		*Tps-b*																
(4) *A. thaliana* Myrcene/Ocimene S.	**42**	**36**	**50**	100																	
(5) *Salvia officinalis* (+)-Sabinene S.	**44**	**34**	**37**	**38**	100																
(6) *Mentha longifolia* (-)-Limonene S.	**42**	**38**	**38**	**38**	**49**	100															
(7) *Artemisisa annua* Epi-Cedrol S.	28	25	25	25	26	25	100														
(8) *Lycopersicon esculentum* Vespiradiene S.	26	24	22	22	24	24	**33**	100													
(9) *Nicotiana tobacum* 5-epi-Aristolochene S.	32	29	27	27	29	28	**38**	**65**	100		*Tps-a*										
(10) *Gossypium arboreum* δ-Cadinene S.	31	30	28	27	29	28	**39**	**40**	**47**	100											
(11) *Rosa hybrida* Germacrene D S.	32	27	31	30	28	28	**40**	**39**	**44**	**52**	100										
(12) *Mentha x piperita E*-β-Farnesene S.	26	25	26	24	25	23	**31**	**29**	**37**	**33**	**31**	100									
(13) *Abies grandis* (-)-Camphene S.	28	26	26	25	28	26	25	21	24	27	27	21	100								
(14) *Abies grandis* (-)-Pinene S.	28	26	25	24	27	27	25	23	26	28	25	22	**74**	100							
(15) *Abies grandis* Myrcene S.	26	24	23	23	25	25	23	21	23	25	25	22	**65**	**69**	100		*Tps-d*				
(16) *Picea abies* (+)-3-Carene S.	27	26	25	23	26	25	22	21	24	25	26	21	**64**	**67**	**66**	100					
(17) *Abies grandis* (-)-Limonene S.	27	25	25	24	26	25	24	20	23	25	25	21	**61**	**61**	**64**	**64**	100				
(18) *Anthirrhinum majus* ama1e20	27	24	25	25	22	26	24	22	22	25	24	25	23	24	22	22	23	100			
(19) *Anthirrhinum majus* ama0c15	27	24	25	25	22	26	24	22	22	25	24	25	23	24	22	22	23	**97**	100		*Tps-g*
(20) *Anthirrhinum majus* ama0a23	26	24	24	23	22	25	24	21	22	25	24	25	22	23	21	21	22	**90**	**91**	100	
(21) *A. thaliana* TPS14 (At1g61680)	25	25	26	24	23	23	25	25	23	24	26	21	19	19	19	21	20	**34**	**34**	**33**	100

Figure 3. Pair-Wise Percentage Identity of Deduced Amino Acid Sequences of Snapdragon TPS–Like Clones with TPS from Other Species, Including Members of the *Tps-a*, *Tps-b*, and *Tps-d* Subfamilies.

duced two monoterpenes, (*E*)-β-ocimene and myrcene, constituting 80 and 20% of enzyme products, respectively, along with minor amounts of (*Z*)-β-ocimene (Figure 7).

Tissue-Specific, Developmental, and Rhythmic Gene Expression of Monoterpene Synthases

To determine if these three monoterpene synthase genes are expressed with spatial and temporal patterns correlated with floral scent emission, we analyzed monoterpene synthase gene expression in snapdragon flower tissues. Total RNA was isolated from leaves and different floral parts of 3-day-old snapdragon flowers (sepals, pistils, stamens, and different regions of the corolla: the upper petal lobes, the lower petal lobes, and the tube) and used in RNA gel blot analysis. Because of the high sequence similarity between *ama0a23*, *ama0c15*, and *ama1e20* clones, a single monoterpene synthase probe derived from *ama1e20* was used initially for all RNA gel blot analyses. The highest level of monoterpene synthase gene expression was found in the upper and lower lobes of petals (Figure 8A), the parts of the flower that were shown previously to be primarily responsible for scent production and emission in snapdragon (Dudareva et al., 2000). A very low level of transcripts was detected in the tube and stamens. No detectable signals were found in pistils, sepals, and leaf tissues.

Because the signals detected in this RNA gel blot experiment could represent a sum of transcripts for all three isolated monoterpene synthases, the contribution of each gene to the total expression level was analyzed further by reverse transcriptase (RT)–PCR using gene-specific primers. When total RNA isolated from upper and lower petal lobes was used in RT-PCR, different levels of expression were found for *ama0a23*, *ama0c15*, and *ama1e20* (Figure 8B). Although *ama0a23* [(*E*)-β-ocimene synthase] and *ama0c15* (myrcene synthase) genes were expressed at similarly high levels, expression of *ama1e20* (myrcene synthase) was very low and detectable only after overexposure of the autoradiographs presented in Figure 8B. According to quantitative RT-PCR analysis, 60% of the TPS hybridization signal obtained by RNA gel blot analysis (Figures 8A and 9) was attributed to the expression of *ama0c15* and 40% of the signal was attributed to *ama0a23*. This ratio of gene expression was stable during flower development and during a light/dark cycle. *ama1e20* did not contribute significantly to monoterpene synthase expression.

To examine the steady state levels of monoterpene synthase mRNA in upper and lower petal lobes during flower development, total RNA was extracted from the petal lobes of mature flower buds at 1 day before anthesis and from open flowers at 1 to 12 days after anthesis (Figure 9A). A plot showing the changes in the relative amounts of transcripts for monoterpene synthases during the life span of the flower, normalized to equal amounts of 18S rRNA, is presented in Figure 9B. Monoterpene synthase mRNA was detected first in mature flower buds, and its level increased until it peaked on day 4 after an-

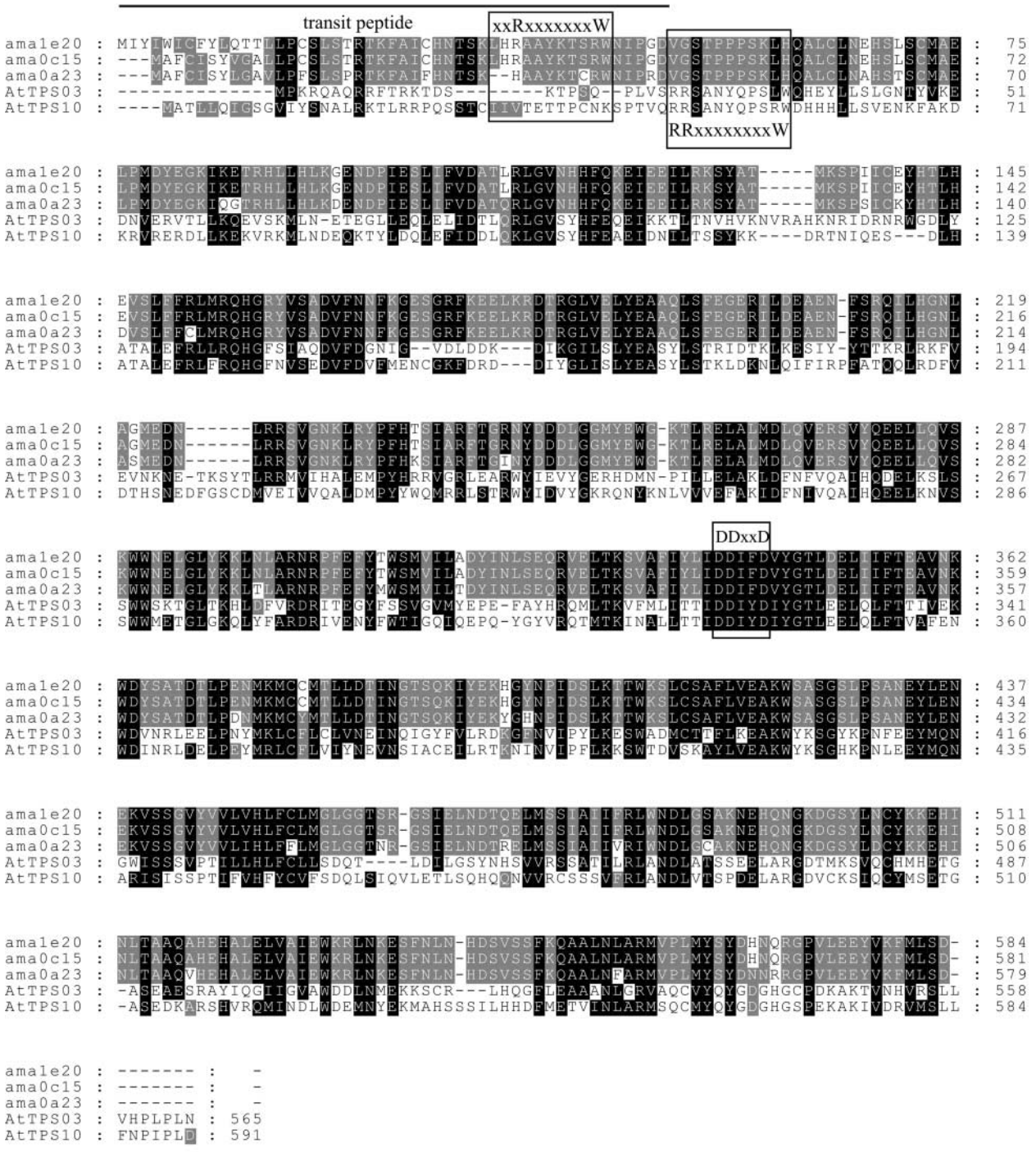

Figure 4. Alignment of Snapdragon Monoterpene Synthases.

Amino acid sequence alignment of snapdragon *ama1e20* (myrcene synthase), *ama0c15* (myrcene synthase), and *ama0a23* [(*E*)-β-ocimene synthase] predicted proteins with the functionally similar monoterpene synthases AtTPS03 (At4g16740) [(*E*)-β-ocimene synthase] and AtTPS10 (At2g24210) (myrcene/ocimene synthase) from Arabidopsis. Residues shaded black indicate conserved residues (identical in at least four of five sequences shown), and residues shaded gray are identical in at least two of five sequences shown. A horizontal line indicates the putative N-terminal transit peptide region. The RRx_8W motif and the DDxxD motif, which are highly conserved in plant monoterpene synthases and have known functions in the TPS reaction mechanism, are shown. The RRx_8W motif is missing in the three snapdragon sequences but conserved in Arabidopsis TPS of similar function. Snapdragon TPS contain a similar motif, $xxRx_6W$, although in a position that is within the proposed transit peptide and not conserved with the position of the RRx_8W motif.

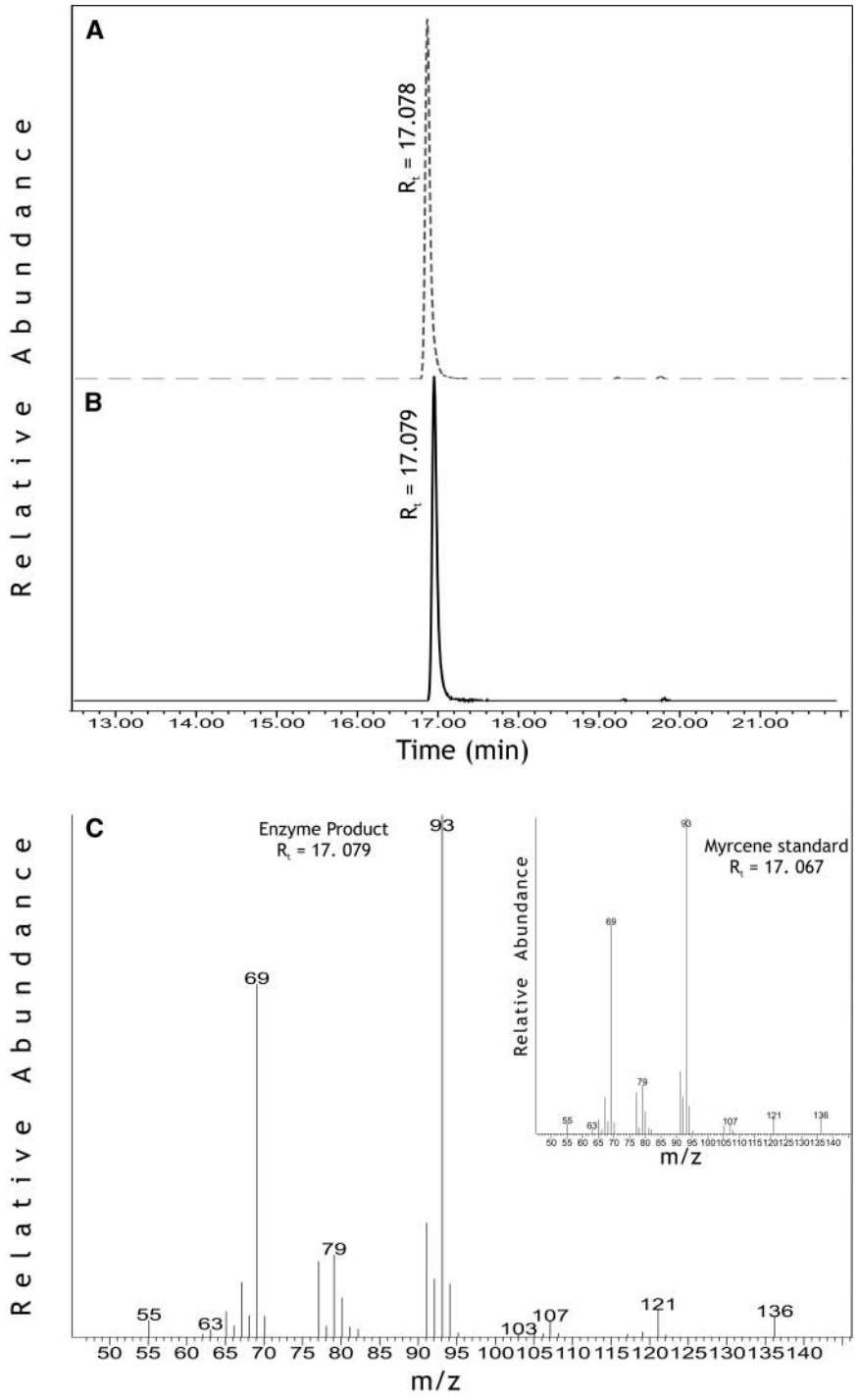

Figure 5. GC-MS of the Monoterpene Products Formed from GPP by *ama0c15* and *ama1e20* Enzymes.

(A) and **(B)** Total ion chromatographs are shown for *ama0c15* **(A)** and *ama1e20* **(B)**. The retention times for the single product formed by each of these two enzymes were identical. Mass spectra of these peaks were identical.

(C) The mass spectrum of the *ama1e20* product is shown with the spectrum of an authentic myrcene standard.

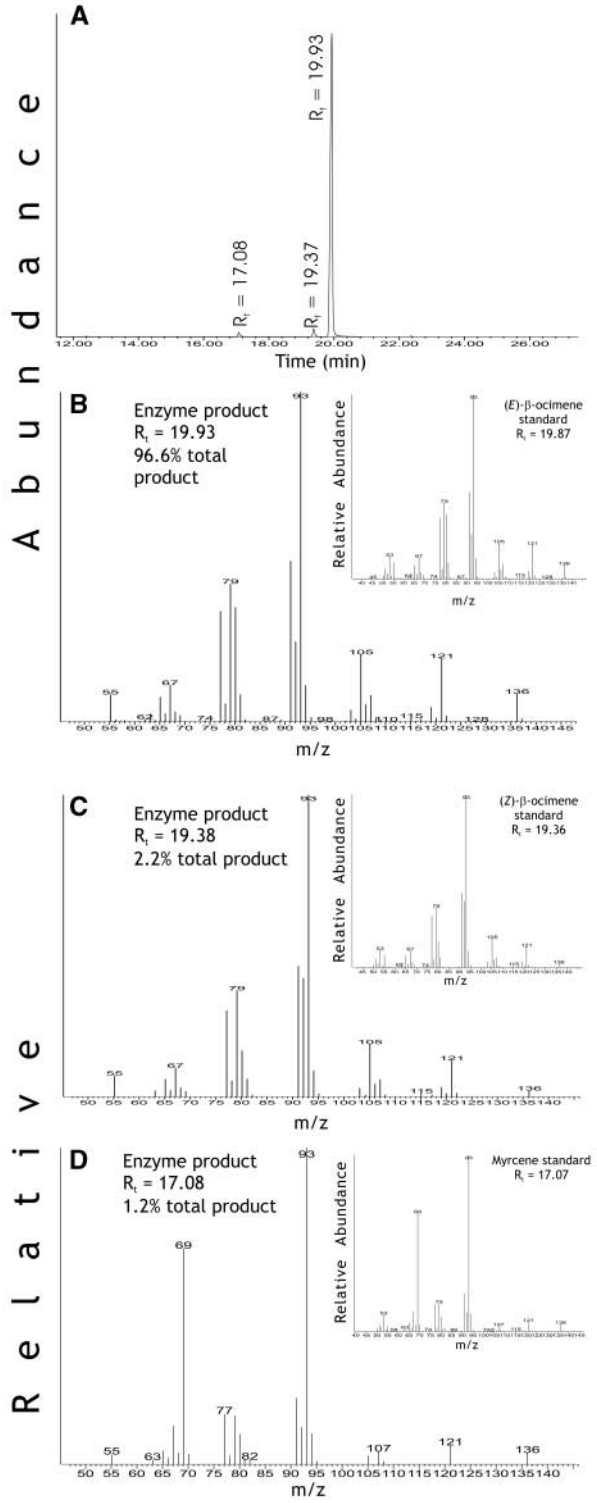

Figure 6. GC-MS Analysis of the Products Formed from GPP by *ama0a23* Enzyme.

(A) Total ion chromatograph of the major and minor products formed by *ama0a23*.

(B) to **(D)** Mass spectra are shown for three peaks presented in order of decreasing abundance with the mass spectra of authentic standards. m/z, mass-to-charge ratio; R_t, retention time.

(B) Mass spectrum of peak retention time 19.93 and (*E*)-β-ocimene standard.

(C) Mass spectrum of peak retention time 19.38 and (*Z*)-β-ocimene standard.

(D) Mass spectrum of peak retention time 17.08 and (*E*)-β-myrcene standard.

thesis (Figures 9A and 9B). Over the next 3 days (days 5 to 7), mRNA levels declined sharply by 40% and decreased slowly thereafter (Figures 9A and 9B).

Next, we determined whether the oscillations in myrcene and (*E*)-β-ocimene emissions during a light/dark cycle (Figure 1B) were the function of rhythmic regulation of the corresponding gene expression. Accumulation of mRNA was examined in upper and lower petal lobes at nine time points during a 27-h interval (Figure 9C). The mRNA levels were quantified and normalized for any loading differences, and the relative values are shown in Figure 9D. We found only slight variations in monoterpene synthase mRNA levels during the daily light/dark cycle. Levels of transcripts for monoterpene synthases increased during the light period, and their maximum accumulation was detected at ~3 PM; they then declined at least twofold during the dark period (12 AM), showing a weak diurnal oscillation pattern. The rhythmic pattern of mRNA accumulation was retained under continuous dark (Figure 9E), suggesting that the cyclic expression of monoterpene synthases is under circadian control. Although changes in transcript levels may not directly determine protein levels or enzyme activities due to possible post-transcriptional, post-translational, or enzyme-regulatory mechanisms, the positive correlation between transcript levels and volatile emission suggests that changes in transcript level are an important determinant of scent production.

DISCUSSION

Monoterpene Synthases Involved in Snapdragon Floral Scent Biosynthesis

Monoterpene compounds, such as (*E*)-β-ocimene and myrcene, contribute significantly to the floral odors of numerous plant species (Knudsen et al., 1993). (*E*)-β-Ocimene constitutes 87% of the scent of the orchid *Laelia anceps* (Kaiser, 1993), whereas the scent of *Brugmansia* × *candida*, a member of the Solanaceae, contains as much as 52% (*E*)-β-ocimene (Kite and Leon, 1995). In snapdragon, the monoterpene fraction of the floral scent bouquet is dominated by (*E*)-β-ocimene and myrcene, which account for 20 and 8% of total floral volatiles, respectively (Dudareva et al., 2000). Developmental and diurnal rhythmic emissions of these two acyclic monoterpenes follow similar patterns, with (*E*)-β-ocimene approximately twofold to fourfold more abundant than myrcene (Figure 1). Therefore, it is possible that the coordination of the formation and emission of myrcene and (*E*)-β-ocimene is the result of the action of a single multiproduct monoterpene synthase. A myrcene/ocimene

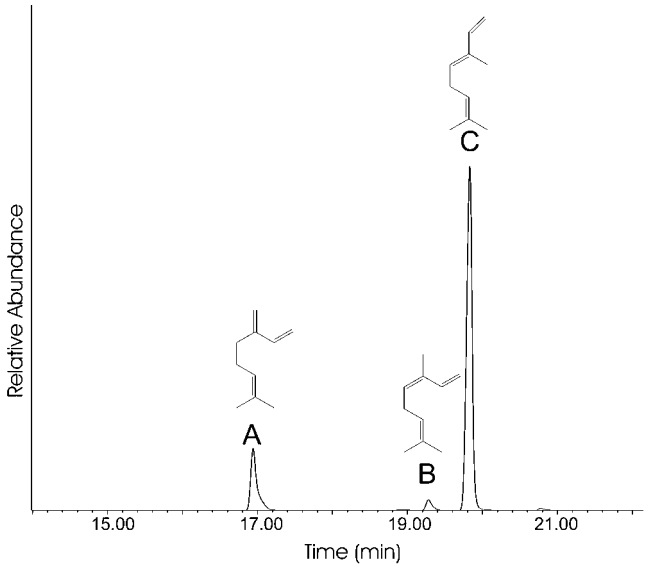

Figure 7. Product Profile of Monoterpene Synthase Activity from Snapdragon Flowers.

GC of the products formed from GPP by native snapdragon monoterpene synthase enzyme activity extracted from upper and lower lobes of flowers at day 5 after anthesis. Peaks are myrcene (A), (*Z*)-β-ocimene (B), and (*E*)-β-ocimene (C).

synthase (AtTPS10 [At2g24210]) has been characterized in Arabidopsis that converts geranyl diphosphate into myrcene (56% of total hydrocarbon product), (*E*)-β-ocimene (20%), and small amounts of cyclic monoterpenes (each <5%) (Bohlmann et al., 2000b). On the other hand, specialized monoterpene synthases with a single major product also are known. For example, Arabidopsis AtTPS03 (At4g16740) produces mainly (*E*)-β-ocimene (Fäldt et al., 2003a), whereas the only product of myrcene synthase from grand fir is myrcene (Bohlmann et al., 1997).

As part of an ongoing EST-based effort to discover genes of floral scent in snapdragon, we isolated three new monoterpene synthase genes and identified them using a biochemical, functional approach as myrcene (*ama1e20* and *ama0c15*) and (*E*)-β-ocimene (*ama0a23*) synthases. The products of these synthases are the two dominant isoprenoids of snapdragon floral fragrance. These three monoterpene synthases are highly similar to each other and encode proteins of 66 to 67 kD with a pI value near 6.0, which is similar to that of other known monoterpene synthases (Bohlmann et al., 1998; Wise and Croteau, 1999). *ama1e20* and *ama0c15* deduced proteins are almost identical except for the N-terminal 13 amino acids (Figure 4). Two independent methods (5′ RACE and cDNA library screening) verified that these clones are not cDNA cloning artifacts of the same gene but represent different genes or allelic variations of the same gene. Despite the differences within the N-terminal amino acids, *ama1e20* and *ama0c15* both encode functional myrcene synthases. This finding supports earlier data that N-terminal regions of up to 60 to 70 amino acids of monoterpene synthases are not critical for enzyme catalytic function (Williams et al., 1998; Bohlmann et al., 1999). *ama0a23* [(*E*)-β-ocimene synthase] also is highly similar (92% identical) to *ama1e20* and *ama0c15*, yet it is specialized for a different biochemical function. This small family of three monoterpene synthases from snapdragon demonstrates that the function of *TPS* ESTs cannot be predicted based on sequence. The snapdragon *TPS* genes are most likely derived from a common ancestor via gene duplication and functional radiation, similar to the *TPS* genes in Arabidopsis and conifers (Bohlmann et al., 1999; Aubourg et al., 2002). The precise structural features that determine the product specificity of monoterpene synthases remain to be deciphered, and such knowledge will contribute to our understanding of the adaptive evolution of floral scent phenotypes.

Interestingly, one of the myrcene synthase genes, *ama1e20*, is not expressed at significant levels in snapdragon petal tissues, indicating that only *ama0c15* (myrcene synthase) and *ama0a23* [(*E*)-β-ocimene synthase] contribute to terpene synthase transcript accumulation and, correspondingly, to floral myrcene and (*E*)-β-ocimene emission (Figures 8 and 9). The myrcene synthase *ama0c15* contributes 1.5 times more (60%) than the (*E*)-β-ocimene synthase *ama0a23* (40%) to the total monoterpene transcript levels in upper and lower petal lobes of

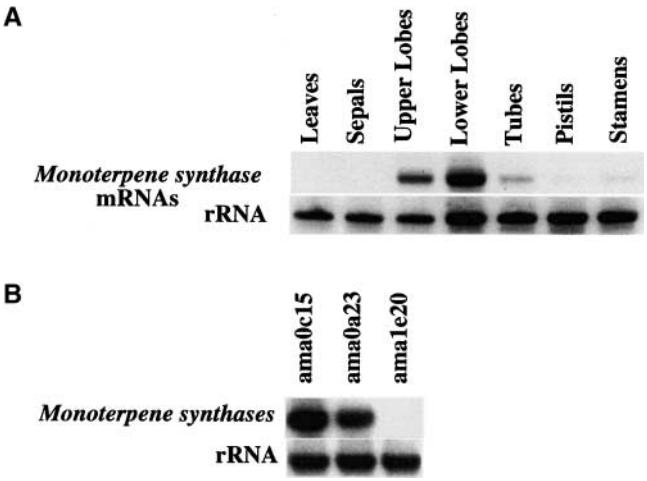

Figure 8. Tissue Specificity of Snapdragon Monoterpene Synthase Gene Expression.

(A) RNA gel blot of total RNA (5 μg per lane) isolated from young leaves, sepals, pistils, stamens, upper and lower petal lobes, and tubes of 3-day-old snapdragon flowers. The top gel represents the results of hybridization with a coding region of the monoterpene synthase genes derived from *ama1e20* as a probe. The length of the monoterpene synthase mRNA was estimated as 2.8 kb using RNA molecular markers in an adjacent lane. Autoradiography was performed for 48 h. The blot was rehybridized with an 18S rRNA probe (bottom gel) to standardize samples.
(B) Contribution of each monoterpene synthase to total monoterpene synthase gene expression. RT-PCR with gene-specific primers was performed on RNA isolated from upper and lower petal lobes of 6-day-old snapdragon flowers. Relative expression was estimated after hybridization of RT-PCR products with the same gene probe used in the RNA gel blot analysis **(A)**. Hybridization signals were analyzed using a Storm 860 PhosphorImager and ImageQuant software (Molecular Dynamics).

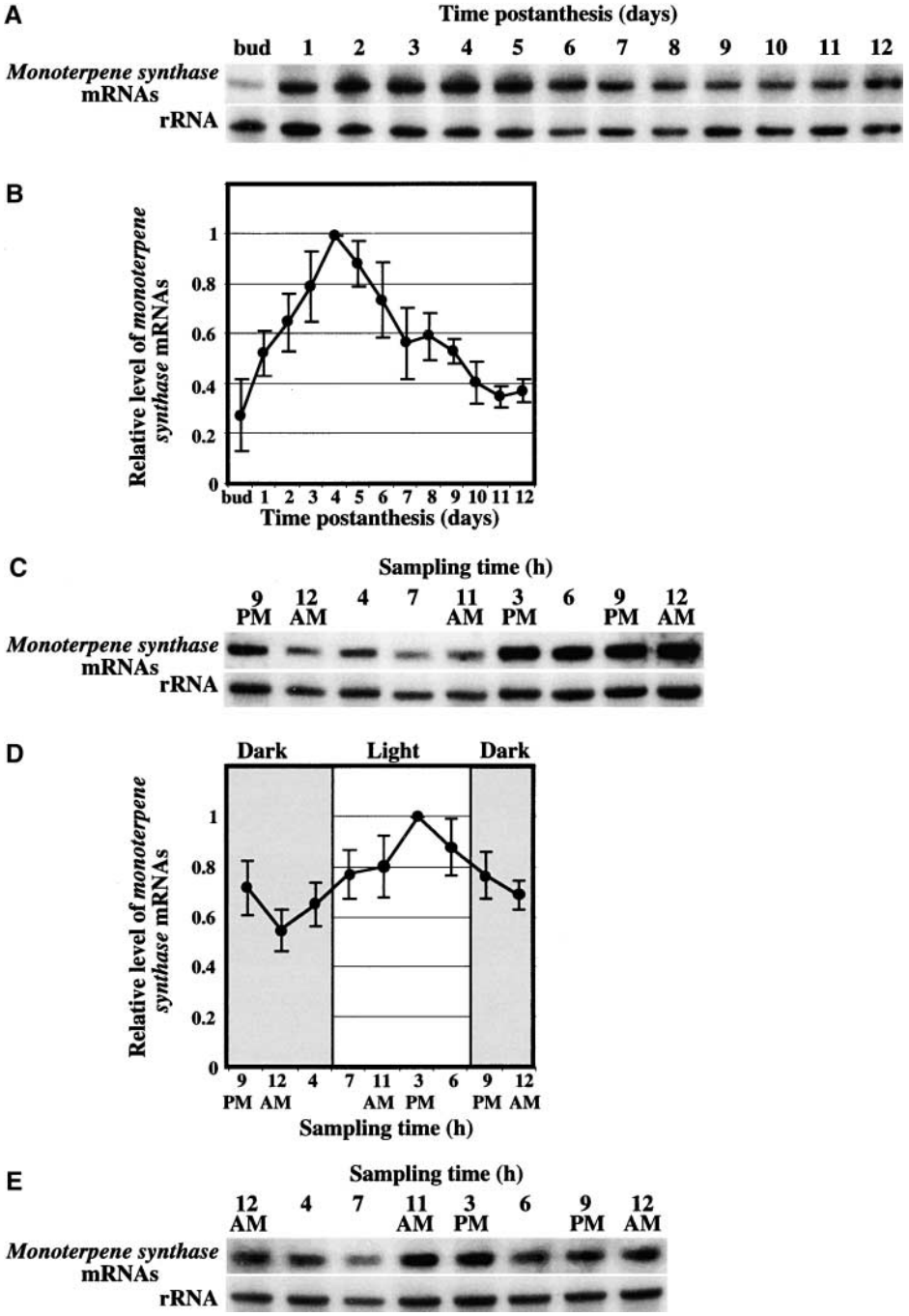

Figure 9. Developmental and Rhythmic Changes in Steady State Monoterpene Synthase mRNA Levels in Upper and Lower Lobes of Snapdragon Petals.

(A) Representative RNA gel blot hybridization with mRNA isolated from upper and lower petal lobes at different stages of development from mature flower buds to day 12 after anthesis. Each lane contained 5 μg of total RNA. Autoradiography was performed overnight. The blots were rehybridized with an 18S rRNA probe (bottom gel) to standardize samples.

(B) Plot of the variations in levels of monoterpene synthase mRNAs in upper and lower petal lobes throughout the life span of the flower. Values were obtained by scanning RNA gel blots with a PhosphorImager and corrected by standardizing for the amounts of 18S rRNA measured in the same runs. The maximum transcript level was taken as 1. Each point is the average of four different experiments (including the one shown in **[A]**). Standard error values are indicated by vertical bars.

(C) RNA gel blot analysis of steady state monoterpene synthase mRNA levels in snapdragon petals during a normal light/dark cycle. Total RNA was isolated from upper and lower petal lobes of 3-day-old flowers at the time points indicated at top, and 5 μg of total RNA was loaded in each lane. Autoradiography was performed overnight. The blot was rehybridized with an 18S rRNA probe (bottom gel) to standardize samples.

snapdragon flowers (Figure 8B). However, snapdragon flowers emit more (*E*)-β-ocimene relative to myrcene (20 and 8% of total floral volatiles, respectively), and monoterpene synthase enzyme activities form a mixture of monoterpenes that is high in (*E*)-β-ocimene (~80% of native enzyme product) and low in myrcene (~20%), along with minor amounts of (*Z*)-β-ocimene (Figure 7). Together, these data imply that the snapdragon monoterpene floral scent profile may be regulated at translational and/or post-translational levels of the corresponding monoterpene synthases. Different rates of protein synthesis and proteolytic turnover and/or differences in protein modifications or the kinetic properties of the two monoterpene synthases could influence the ratio of (*E*)-β-ocimene and myrcene emitted from floral tissues. Secondary modification of monoterpene olefins (e.g., oxidation/glycosylation) or sequestration also could contribute to the monoterpene emission profile. Indeed, transgenic expression of linalool synthase in petunia flowers resulted in the accumulation of monoterpenol conjugates, leading to a weak emission of linalool (Lücker et al., 2001).

Snapdragon Monoterpene Synthases Lack the Conserved RRx_8W Motif

An interesting feature of all three snapdragon monoterpene synthases is the lack of the RRx_8W motif (Figure 4), which is characteristic of other monoterpene synthases of the angiosperm *Tps-b* group and the gymnosperm *Tps-d* group (Bohlmann et al., 1998, 1999; Aubourg et al., 2002). In the formation of the cyclic monoterpene (−)-*4S*-limonene catalyzed by *Mentha spicata* limonene synthase, the double-Arg element of the RRx_8W motif is involved in the diphosphate migration step to yield *3S*-linalyl diphosphate (LPP) (Williams et al., 1998). LPP is the proposed essential, enzyme-bound intermediate for monoterpene cyclization (Wise and Croteau, 1999). However, the formation of acyclic myrcene and ocimene may not require the isomerization of GPP to an LPP intermediate but could be formed directly from GPP after cleavage of the diphosphate group without covalent readdition of the diphosphate moiety (Bohlmann et al., 1999). The absence of any cyclic monoterpenes in the product fraction of snapdragon myrcene and (*E*)-β-ocimene synthases could be attributable to the lack of an intact RRx_8W motif. The RRx_8W motif also is missing in two other monoterpene synthases of known function, *Clarkia* LIS (Dudareva et al., 1996) and Arabidopsis AtTPS14 (At1g61680) (Aubourg et al., 2002; Chen et al., 2003). *Clarkia* LIS and Arabidopsis AtTPS14 both encode synthases specialized for the formation of the acyclic monoterpene alcohol linalool from GPP (Dudareva et al., 1996; Chen et al., 2003).

Snapdragon Monoterpene Synthases Are Members of a New *Tps-g* Subfamily

Recent phylogenetic analysis of the deduced amino acid sequences of isolated plant terpenoid synthases revealed six TPS gene subfamilies, designated *Tps-a* through *Tps-f* (Bohlmann et al., 1998). The three newly isolated snapdragon monoterpene synthases do not cluster with functional homologs of the *Tps-b* family of angiosperm monoterpene synthases and the *Tps-d* family of conifer monoterpene synthases (Bohlmann et al., 1998; Aubourg et al., 2002), despite sharing overall sequence similarity (Figure 10). Moreover, among all functionally identified plant TPS, the snapdragon ocimene and myrcene synthases closely resemble Arabidopsis AtTPS14 (At1g61680), a TPS that previously represented an isolated branch of the plant TPS family (Aubourg et al., 2002). Together, the snapdragon monoterpene synthases *ama0c15*, *ama0a23*, and *ama1e20* and Arabidopsis AtTPS14 (At1g61680) define a new subfamily of the TPS family designated the *Tps-g* group (Figure 10).

In addition to overall high sequence identity within this new subfamily and low sequence relatedness with the TPS of other subfamilies, monoterpene synthases of this new *Tps-g* group lack the RRx_8W motif, which is a characteristic feature of the *Tps-d* and *Tps-b* monoterpene synthases. All four functionally characterized members of the *Tps-g* group produce acyclic monoterpenes, and surprisingly, all of them, including Arabidopsis AtTPS14 (Chen et al., 2003), contribute to floral volatiles. Members of the *Tps-f* subfamily (*Clarkia* linalool synthase and Arabidopsis AtTPS04 [At1g61120; unknown function]) and members of the *Tps-e* and *Tps-c* groups (kaurene synthases and copalyl diphosphate synthase, respectively) contain an additional 200–amino acid motif of unknown function that is missing in the newly identified *Tps-g* members (Bohlmann et al., 1998; Trapp and Croteau, 2001; Aubourg et al., 2002). Moreover, this new *Tps-g* subfamily is clearly separated, by sequence and function, from the *Tps-a* group, which contains angiosperm sesquiterpene and diterpene synthases (Figure 10).

Coordinated Circadian Rhythmicity, Tissue Specificity, and Developmental Control of Isoprenoids and Phenylpropanoids in Snapdragon Flowers

Previously, we showed that the main sites of the biosynthesis of methylbenzoate, a major phenylpropanoid floral scent com-

Figure 9. (continued).

(D) Plot of the variations in monoterpene synthase mRNA levels in upper and lower petal lobes during a normal light/dark cycle. Values were obtained by scanning RNA gel blots (including the one shown in **[C]**) with a PhosphorImager and corrected by standardizing for the amounts of 18S rRNA measured in the same runs. The maximum transcript level was taken as 1. Each point is the average of three independent experiments (including the one shown in **[B]**). Standard error values are indicated by vertical bars. Shaded and unshaded areas correspond to dark and light periods, respectively.
(E) RNA gel blot analysis of steady state monoterpene synthase mRNA levels in snapdragon flowers exposed to continuous dark. Total RNA was isolated from upper and lower petal lobes of 5-day-old flowers exposed to the second constant dark cycle at the time points indicated at top, and 5 μg of total RNA was loaded in each lane. The blot was rehybridized with an 18S rRNA probe (bottom gel) to standardize samples.

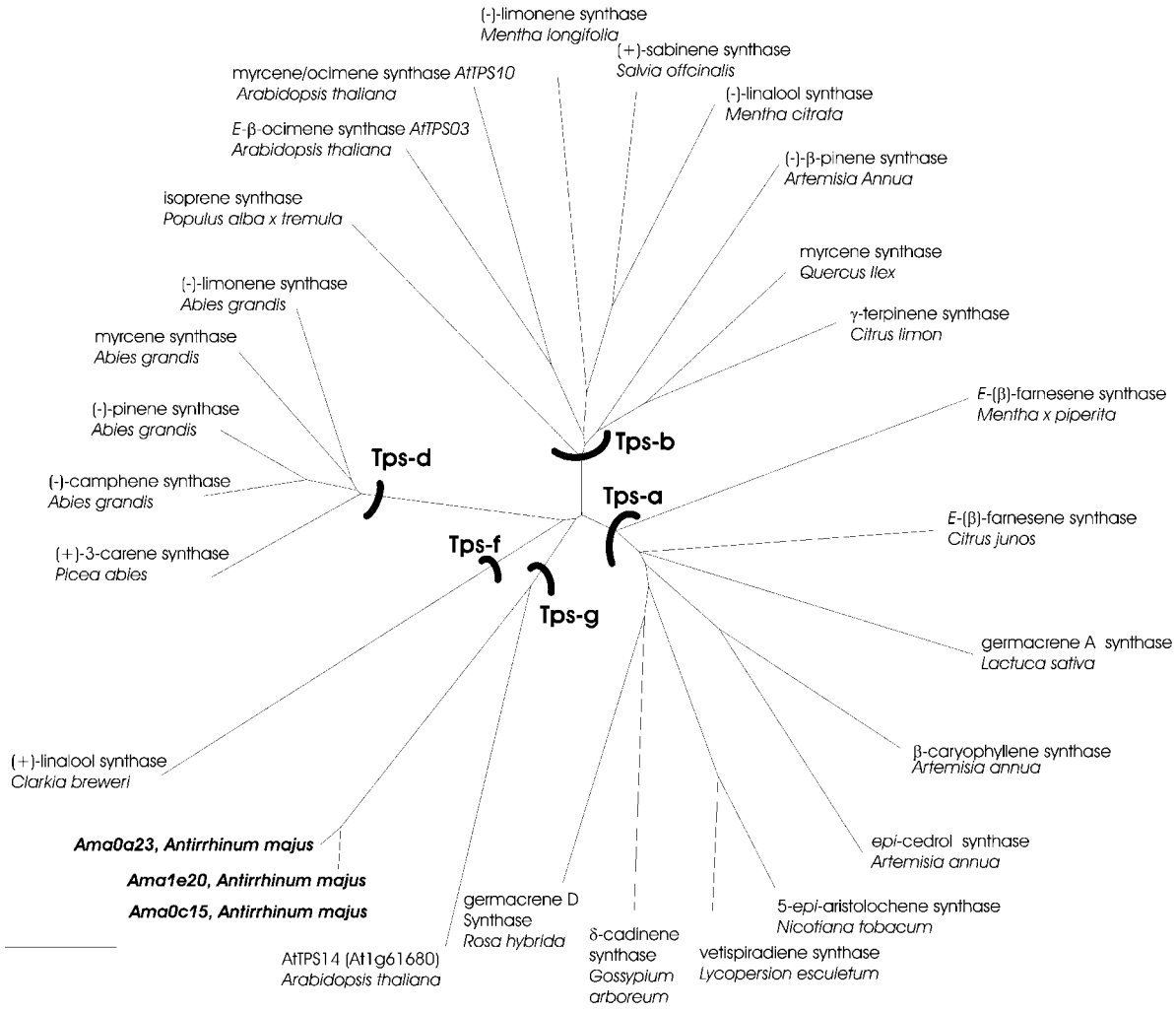

Figure 10. Phylogenetic Tree Illustrating the Relatedness of Subfamilies of the Plant TPS Family, Including the New *Tps-g* Subfamily.

Division into subfamilies is based on cluster analysis (Bohlmann et al., 1998; Aubourg et al., 2002). Subfamily *Tps-a* consists of sesquiterpene synthases and diterpene synthases of angiosperm secondary metabolism; *Tps-b* comprises the monoterpene synthases from angiosperms that contain the RRx_8W motif; *Tps-d* contains gymnosperm TPS; *Tps-f* includes linalool synthase from *Clarkia* and Arabidopsis AtTPS04 (At1g61120, unknown function) (Aubourg et al., 2002). The new *Tps-g* subfamily was defined to account for the monoterpene synthase genes *ama0c15*, *ama1e20*, and *ama0a23* from snapdragon together with Arabidopsis AtTPS14 (At1g61680), which do not belong to the previously characterized groups *Tps-a* through *Tps-f* based on overall sequence relatedness. Members of the *Tps-g* subfamily lack the RRx_8W motif that is characteristic of all functionally characterized monoterpene synthases of the angiosperm *Tps-b* and the gymnosperm *Tps-d* groups. Sequence analysis was performed using CLUSTAL X, and the nearest neighbor-joining method was used to create trees. TreeView was used to visualize the resulting trees (Page, 1996). Only a subset of the known plant TPS is shown in this tree. Subfamilies *Tps-c* (copalyl diphosphate synthases) and *Tps-e* (kaurene synthases) are not shown.

ponent of snapdragon, are the upper and lower petal lobes, which make almost equal contributions to the whole flower fragrance (Dudareva et al., 2000). Here, we have shown that the production and emission of the other two main fragrance compounds, the monoterpenes myrcene and (*E*)-β-ocimene, also occur in the upper and lower petal lobes, where high levels of monoterpene synthase gene expression have been found (Figure 8A). Emissions of these monoterpene compounds follow very similar diurnal rhythms controlled by a circadian clock (Figures 1B and 2) that match the rhythmic emission of methylbenzoate (Kolosova et al., 2001a), indicating that two apparently separate metabolic pathways are regulated coordinately by a circadian clock to yield diurnal emission of a complex mixture of floral fragrance derived from the isoprenoid and phenylpropanoid pathways.

Similar to *BAMT* mRNA, monoterpene synthase mRNA levels oscillate, with a maximum at ~3 PM before declining at least twofold during the dark period (12 AM) (Figures 9C and 9D), showing strong correlation with corresponding monoterpene emission (Figure 1B). Rhythmic fluctuations in mRNA levels continue in constant dark (Figure 9E), suggesting that, like *BAMT* mRNA, a free-running internal circadian clock regulates the monoterpene

synthase mRNA abundance. Moreover, like *BAMT* mRNA, the steady state mRNA levels of monoterpene synthases in petals are regulated developmentally, peaking on day 4 after anthesis (Figures 9A and 9B), 1 to 2 days ahead of maximum emission (Figure 1A). These results indicate that the emission of phenylpropanoid and isoprenoid volatiles in snapdragon is under similar or identical developmental and diurnal control, as was shown in this study for monoterpenes and previously for methylbenzoate (Dudareva et al., 2000; Kolosova et al., 2001a).

Overall, these findings suggest that emission of a composite floral scent bouquet in snapdragon is regulated upstream of individual metabolic pathways, thus coordinating the emission of phenylpropanoids and isoprenoids. This regulation includes the coordinate expression of genes that encode enzymes involved in the final steps of scent biosynthesis (Figure 9) (Dudareva et al., 2000; Kolosova et al., 2001a). However, the level of scent biosynthetic enzymes is not the only limiting factor, and the target for the regulation of scent production might include the level of supplied substrate in the cell. Although the involvement of benzoic acid in the regulation of rhythmic and developmental methylbenzoate emission has been shown (Dudareva et al., 2000; Kolosova et al., 2001a), the role of GPP in the regulation of monoterpene emission remains to be determined. The biochemical characterization of myrcene and (*E*)-β-ocimene synthases also will provide further information regarding the competition of these two enzymes for the same substrate. The possibility that the level of emitted monoterpenes is regulated at the translational/post-translational level or by the modification of monoterpenes cannot be excluded.

METHODS

Plant Material and Headspace Analysis of Floral Volatiles

Snapdragon (*Antirrhinum majus*) cv Maryland True Pink (Ball Seed, West Chicago, IL) was grown under standard greenhouse conditions as described previously (Dudareva et al., 2000). For the headspace collections of floral volatiles, plants were placed in growth chambers (model E8; Conviron, Asheville, NC) with a 25/20°C (light/dark) temperature cycle, a RH of 40%, and a 12-h photoperiod with light intensity of 350 $\mu mol \cdot m^{-2} \cdot s^{-1}$ for a normal day/night cycle and 100 $\mu mol \cdot m^{-2} \cdot s^{-1}$ for the experiments in continuous light. Emitted volatiles were determined by headspace analysis as described previously (Raguso and Pichersky, 1995; Raguso and Pellmyr, 1998) at 24-h intervals for developmental emission and at seven time points during a 24-h period for rhythmic emission. Trapped floral scent compounds were analyzed by gas chromatography–mass spectrometry (GC-MS) with a FinniganMAT GCQ instrument (Thermoquest, San Jose, CA) and by GC with an Agilent 6890 series gas chromatograph (Agilent Technologies, Palo Alto, CA) as described previously (Dudareva et al., 2000; Kolosova et al., 2001a). Quantification was based on flame ionization detector peak areas and the internal standard. Ten microliters of a 0.03% (v/v) solution of toluene in hexane was added to each sample as an internal standard. Specific correction factors were developed from the myrcene and (*E*)-β-ocimene (Aldrich, Milwaukee, WI) standard curves and applied to peak areas of monoterpenes in samples.

Substrates, Standards, and Reagents

1-^{3}H-Geranyl diphosphate (GPP) (3.7 kBq/mol), 1-^{3}H-farnesyl diphosphate (3.7 kBq/mol), and 1-^{3}H-geranylgeranyl diphosphate (1.2 kBq/mol) were from American Radiolabeled Chemicals (St. Louis, MO). Unlabeled GPP (1 mg/mL) was from Echelon Research Laboratories (Salt Lake City, UT). Terpenoid standards, other chemicals, and reagents were purchased from Sigma Chemical Co., Fluka Chemical Co., or Aldrich Chemical Co. unless noted otherwise.

EST Sequencing, Rapid Amplification of cDNA Ends, and cDNA Library Screening

A λ-ZAPII cDNA library was constructed from mRNA isolated from upper and lower petal lobes of 1- to 5-day-old snapdragon flowers according to the manufacturer's protocol (Stratagene, La Jolla, CA) (Dudareva et al., 2000). The titer of the unamplified library was 1.1×10^6 plaque-forming units. This primary library was amplified, and the amplified library had a titer of 1.5×10^{10} plaque-forming units. Mass excision of pBluescript SK− phagemids (Stratagene) from the amplified library resulted in a stock that was used for plating and random colony picking for DNA sequencing. The inserts were partially sequenced from one end using T3 primer. To isolate full-length cDNA clones, a cDNA library was screened with *ama1e20* probe under high-stringency conditions, as described by Dudareva et al. (1996). Rapid amplification of cDNA ends was performed using the First Choice RLM-RACE system (Ambion, Austin, TX) according to the manufacturer's instructions.

Sequence Analysis

Sequence analysis was performed using programs from the Lasergene DNA-Star Package version 5, CLUSTAL X (http://www-igbmc.u-strasbg.fr/BioInfo/ClustalX) and Genedoc (http://www.psc.edu/biomed/genedoc). Sequence relatedness was analyzed using CLUSTAL X and the neighbor-joining method, and the unrooted tree was visualized using Treedraw (http://taxonomy.zoology.gla.ac.uk/rod/treeview.html; Page, 1996).

Functional Expression of Monoterpene Synthases in *Escherichia coli* and Enzyme Assays

Subcloning and functional expression of *ama1e20*, *ama0c15*, and *ama0a23* in *E. coli* followed a previously published procedure (Fäldt et al., 2003b). The cDNAs were subcloned into the pET100/D-TOPO expression vector (Invitrogen, Carlsbad, CA) according to the manufacturer's instructions. The *ama1e20* cDNA was amplified by PCR using forward primer 5′-CACCATGATCTATATTTGGATCTGCTTTTATCTCCA-3′ in combination with reverse primer 5′-TGTTTAATCCGACAACATAAACTTGAC-3′; *ama0c15* insert was amplified using primers 5′-CACCATGGCATTTTGCATTAGCTAC-3′ and 5′-TTAATCCGACAACATAAACTTGAC-3′; and *ama0a23* insert was amplified using primers 5′-CACCCTCTTAGGTGCAGTGCTTCC-3′ and 5′-TTAATCCGACAACATAAACTTGAC-3′. PCR was performed in volumes of 100 μL containing 20 mM Tris-HCl, pH 8.8, 10 mM KCl, 10 mM $(NH_4)_2SO_4$, 2 mM $MgSO_4$, 0.1% Triton X-100, 10 μg of BSA, 200 μM of each deoxynucleotide triphosphate, 0.1 μM of each primer, 2.5 units of high-fidelity Turbo *Pfu* polymerase (Stratagene), and 2 ng of template DNA. After a denaturing step at 95°C for 2 min, 30 cycles of amplification were performed using the following temperature program in an MJ PTC100 thermocycler (MJ Research, Watertown, MA): 30 s at 95°C, 30 s at 59°C, 2 min at 72°C, followed by a 10-min final extension at 72°C. PCR products were cloned into the pET100/D-TOPO vector, and recombinant plasmids were transformed into *E. coli* TOP10 F′ cells according to the protocol for ligation and transformation (Invitrogen). Plasmids pET-*ama1e20*, pET-*ama0c15*, and pET-*ama0a23* were identified by PCR and purified, inserts were sequenced, and the plasmids were transformed for expression in *E. coli* BL21-CodonPlus(DE3) (Stratagene).

For functional expression, bacterial *E. coli* BL21-CodonPlus(DE3) strains transformed with pET-*ama1e20*, pET-*ama0c15*, or pET-*ama0a23* were grown to A_{600} = 0.5 at 37°C in 5 mL of Luria-Bertani medium supplemented with 20 μg/mL ampicillin. Cultures then were induced by the addition of isopropyl-1-thio-β-D-galactopyranoside to a final concentration of 1 mM and grown for another 12 h at 20°C. Cells were harvested by centrifugation, resuspended in 1 mL of monoterpene synthase buffer (25 mM Hepes, pH 7.2, 10 mM $MnCl_2$, 10% glycerol, and 5 mM DTT), and disrupted by sonication using a Branson Sonifier 250 (Branson Ultrasonic Corp., Danbury, CT) at constant power (5 W) for 10 s. Lysates were cleared by centrifugation, and the resulting supernatants containing the soluble enzyme were assayed for monoterpene, sesquiterpene, and diterpene synthase activity using the appropriate radiolabeled substrates or nonlabeled substrates as described previously (Bohlmann et al., 1997; Peters et al., 2000; Fäldt et al., 2003b).

Enzyme Assays of Snapdragon Native Floral Monoterpene Synthases

Flowers were ground in a chilled mortar with 10 volumes of extraction buffer (50 mM 3-[*N*-morpholino]-2-hydroxypropanesulfonic acid, pH 6.9, 5 mM DTT, 5 mM $Na_2S_2O_5$, 1% [w/v] polyvinylpyrrolidone-40, and 10% glycerol). Extracts were shaken gently for 30 min on ice followed by centrifugation (15,000*g* for 30 min at 4°C). The supernatant was passed through a cell strainer to remove any large particles and frozen at −80°C. To assay monoterpene activity, the protein extract was thawed in water (22°C) and desalted by filter centrifugation (30K Macrosep; Pall Corp., Ann Arbor, MI). Proteins were resuspended in assay buffer (as described for recombinant enzyme assays) and incubated for 2 h with 250 μM GPP. Products of native enzyme assays were purified as described above for recombinant enzymes.

Monoterpene Product Identification by GC-MS

Monoterpene products formed by recombinant or native enzymes were identified by GC-MS analysis on an Agilent 6890 Series GC System coupled to an Agilent 5973 Network Mass Selective Detector (70 eV) using an HP 5 (Agilent Technologies) capillary column (both of which have the following dimensions: 0.25 mm i.d. × 30 m with 25-μm film). The injector was operated splitless at a temperature of 200°C with a column flow of 1 mL He/min. The following temperature program was used: initial temperature of 40°C (2-min hold), increase to 160°C at 3°C/min, 10°C/min ramp to 200°C, followed by a 20°C/min ramp to 300°C (3-min hold). Product identifications were verified using a DB-WAX capillary column (J&W Scientific, Palo Alto, CA) using the same program described above but with a final temperature of 260°C. Monoterpenes were identified by comparing mass spectra using Chemstation software (Agilent Technologies) and Wiley125 MS-library (Wiley Publishing, Hoboken, NJ) and by comparing retention times and mass spectra with those of authentic standards.

RNA Isolation and RNA Gel Blot Analysis

Total RNA was isolated and analyzed as described previously (Dudareva et al., 1996, 1998, 2000; Wang et al., 1997; Kolosova et al., 2001a) from floral tissues and petals at different stages of flower development, nine time points during a daily light/dark cycle, and eight time points during continuous dark conditions. A 1.9-kb EcoRI fragment containing the coding region of the monoterpene synthase genes derived from *ama1e20* was used as a probe in RNA gel blot analysis. Five micrograms of total RNA was loaded in each lane. Hybridization signals were quantified using a Storm 860 phosphor screen (Molecular Dynamics, Sunnyvale, CA), and mRNA transcript levels were normalized to rRNA levels to overcome error in RNA quantitation by spectrophotometry. Multiple independent RNA gel blots were prepared and analyzed for each time point, and a representative time-course profile is presented.

Reverse Transcriptase–PCR

Quantitative reverse transcriptase (RT)–PCR was performed as described previously (Gang et al., 2002) with some modifications. One microgram of total RNA was used to make cDNA using random hexamer primers with the Advantage RT-for-PCR kit according to the manufacturer's instructions (Clontech, Palo Alto, CA). To analyze the contribution of *ama1e20* and *ama0c15* in the expression pattern, two forward gene-specific primers were designed for PCR. These primers amplified products of 800 bp in the 5′ regions of the coding sequences and were as follows: for *ama1e20*, 5′-TATTTGGATCTGCTTTTATCTCC-3′, and for *ama0c15*, 5′-TTGCATTAGCTACGTAGGTGC-3′. The contribution of *ama0c15* and *ama0a23* then was examined using two other forward gene-specific primers, 5′-CATAACACGAGTAAACTACATCG-3′ for *ama0c15* and 5′-TATTTCATAACACGAGTAAACATG-3′ for *ama0a23*, which amplified products of 740 bp. For each PCR, the same reverse conserved primer, 5′-TACTTGCAAATCCATCAGGGC-3′, was used. Reactions were performed in duplicate for 30 cycles with an annealing temperature of 52°C.

Analysis of products obtained by PCR with different amounts of cDNA (5, 10, 15, and 20 μL) showed that product increased linearly. Fifteen microliters of cDNA was chosen as an optimal level for further PCR. To ensure that an equal amount of RNA was used for all samples and that RT reactions were equally effective, PCR was performed with the 18S rRNA gene-specific primers 5′-GATAAAAGGTCGACACGGGCTCTGC-3′ (forward) and 5′-AACGGAATTAACCAGACAAATCGCTCC-3′ (reverse). For rDNA, PCR was performed for 15 cycles at an annealing temperature of 60°C. The amplified products were run on 1.2% agarose gels, blotted onto nitrocellulose membranes (Trans-Blot Transfer Medium; Bio-Rad, Hercules, CA), and hybridized with the corresponding DNA probe, a 1.9-kb EcoRI fragment of *ama1e20* or a 1-kb BamHI-EcoRI fragment of rDNA. Quantitation was performed using a Storm 860 PhosphorImager and ImageQuant software (Molecular Dynamics).

Upon request, all novel materials described in the article will be made available in a timely manner for noncommercial research purposes.

Accession Numbers

The GenBank accession numbers for the sequences mentioned in this article are as follows: *ama0c15*, AY195608; *ama1e20*, AY195609; *ama0a23*, AY195607; AtTPS03 [At4g16740; (*E*)-β-ocimene synthase], AY151086; and AtTPS10 (At2g24210; myrcene/ocimene synthase), AF178535.1.

ACKNOWLEDGMENTS

We thank Gen-ichiro Arimura for assistance and Rodney Croteau for helpful comments. This work was supported by grants to N.D. from the National Science Foundation (Grant MCB-0212802), the Fred Gloeckner Foundation, and the American Floral Endowment and by grants to J.B. from the Natural Sciences and Engineering Research Council of Canada, the Canadian Foundation for Innovation, and British Columbia Knowledge Development Funds. J.F. received fellowships from the Bengt Lundqvist Minne Foundation (Sweden) and the Swedish Foundation for International Cooperation in Research and Higher Education. D.M. is a recipient of a Walter C. Koerner fellowship of the University of British Co-

lumbia. This article is contribution 16,971 from the Purdue University Agricultural Experimental Station.

Received February 3, 2003; accepted March 9, 2003.

REFERENCES

Aubourg, S., Lecharny, A., and Bohlmann, J. (2002). Genomic analysis of the terpenoid synthase (*AtTPS*) gene family of *Arabidopsis thaliana*. Mol. Gen. Genomics **267,** 730–745.

Bohlmann, J., Gershenzon, J., and Aubourg, S. (2000a). Biochemical, molecular genetic and evolutionary aspects of defense-related terpenoid metabolism in conifers. Recent Adv. Phytochem. **34,** 109–150.

Bohlmann, J., Martin, D., Oldham, N.J., and Gershenzon, J. (2000b). Terpenoid secondary metabolism in *Arabidopsis thaliana*: cDNA cloning, characterization, and functional expression of a myrcene/(*E*)-β-ocimene synthase. Arch. Biochem. Biophys. **375,** 261–269.

Bohlmann, J., Meyer-Gauen, G., and Croteau, R. (1998). Plant terpenoid synthases: Molecular biology and phylogenetic analysis. Proc. Natl. Acad. Sci. USA **95,** 4126–4133.

Bohlmann, J., Phillips, M., Ramachandiran, V., Katoh, S., and Croteau, R. (1999). cDNA cloning, characterization, and functional expression of four new monoterpene synthase members of the *Tpsd* gene family from grand fir (*Abies grandis*). Arch. Biochem. Biophys. **368,** 232–243.

Bohlmann, J., Steele, C.L., and Croteau, R. (1997). Monoterpene synthases from grand fir (*Abies grandis*): cDNA isolation, characterization, and functional expression of myrcene synthase, (−)-(*4S*)-limonene synthase, and (−)-(*1S,5S*)-pinene synthase. J. Biol. Chem. **272,** 21784–21792.

Chen, F., Tholl, D., D'Auria, J.C., Farooq, A., Pichersky, E., and Gershenzon, J. (2003). Biosynthesis and emission of terpenoid volatiles from Arabidopsis flowers. Plant Cell **15,** 481–494.

Davis, E.M., and Croteau, R. (2000). Cyclization enzymes in the biosynthesis of monoterpenes, sesquiterpenes, and diterpenes. Top. Curr. Chem. **209,** 53–95.

Dobson, H.E.M. (1994). Floral volatiles in insect biology. In Insect–Plant Interactions, Vol. V, E. Bernays, ed (Boca Raton, FL: CRC Press), pp. 47–81.

Dudareva, N., Cseke, L., Blanc, V.M., and Pichersky, E. (1996). Evolution of floral scent in *Clarkia*: Novel patterns of *S*-linalool synthase gene expression in the *C. breweri* flower. Plant Cell **8,** 1137–1148.

Dudareva, N., D'Auria, J.C., Nam, K.H., Raguso, R.A., and Pichersky, E. (1998). Acetyl CoA:benzyl alcohol acetyltransferase: An enzyme involved in floral scent production in *Clarkia breweri*. Plant J. **14,** 297–304.

Dudareva, N., Murfitt, L.M., Mann, C.J., Gorenstein, N., Kolosova, N., Kish, C.M., Bonham, C., and Wood, K. (2000). Developmental regulation of methyl benzoate biosynthesis and emission in snapdragon flowers. Plant Cell **12,** 949–961.

Dudareva, N., and Pichersky, E. (2000). Biochemical and molecular aspects of floral scents. Plant Physiol. **122,** 627–634.

Fäldt, J., Arimura, G.-i., Gershenzon, J., Takabayashi, J., and Bohlmann, J. (2003a). Functional identification of *AtTPS03* as (*E*)-β-ocimene synthase: A monoterpene synthase catalyzing jasmonate- and wound-induced volatile formation in *Arabidopsis thaliana*. Planta **216,** 745–751.

Fäldt, J., Martin, D., Miller, B., Rawat, S., and Bohlmann, J. (2003b). Traumatic resin defense in Norway spruce (*Picea abies*): Methyl jasmonate-induced terpene synthase gene expression, and cDNA cloning and functional characterization of (+)-3-carene synthase. Plant Mol. Biol. **51,** 119–133.

Gang, D.R., Lavid, N., Zubieta, C., Chen, F., Beuerle, T., Lewinsohn, E., Noel, J.P., and Pichersky, E. (2002). Characterization of phenylpropene *O*-methyltransferases from sweet basil: Facile change of substrate specificity and convergent evolution within a plant *O*-methyltransferase family. Plant Cell **14,** 505–519.

Guterman, I., et al. (2002). Rose scent: Genomics approach to discovering novel floral fragrance-related genes. Plant Cell **14,** 2325–2338.

Kaiser, R. (1993). The Scent of Orchids. (Amsterdam: Elsevier).

Kite, G.C., and Leon, C. (1995). Volatile compounds emitted from flowers and leaves of *Brugmansia* × *candida* (Solanaceae). Phytochemistry **40,** 1093–1095.

Knudsen, J.T., Tollsten, L., and Bergstrom, G. (1993). Floral scents: A checklist of volatile compounds isolated by head-space techniques. Phytochemistry **33,** 253–280.

Kolosova, N., Gorenstein, N., Kish, C.M., and Dudareva, N. (2001a). Regulation of circadian methyl benzoate emission in diurnally and nocturnally emitting plants. Plant Cell **13,** 2333–2347.

Kolosova, N., Sherman, D., Karlson, D., and Dudareva, N. (2001b). Cellular and subcellular localization of *S*-adenosyl-L-methionine:benzoic acid carboxyl methyltransferase, the enzyme responsible for biosynthesis of the volatile ester methyl benzoate in snapdragon flowers. Plant Physiol. **126,** 956–964.

Lücker, J., Bouwmeester, H.J., Schwab, W., Blaas, J., Van der Plas, L.H.W., and Verhoeven, H.A. (2001). Expression of *Clarkia S*-linalool synthase in transgenic petunia plants results in the accumulation of *S*-linalyl-β-D-glucopyranoside. Plant J. **27,** 315–324.

Page, R.D.M. (1996). TREEVIEW: An application to display phylogenetic trees on personal computers. Comput. Appl. Biosci. **12,** 357–358.

Peters, R.J., Flory, J.E., Jetter, R., Ravn, M.M., Lee, H.J., Coates, R.M., and Croteau, R. (2000). Abietadiene synthase from grand fir (*Abies grandis*): Characterization and mechanism of action of the "pseudomature" recombinant enzyme. Biochemistry **39,** 15592–15602.

Pichersky, E., Lewinsohn, E., and Croteau, R. (1995). Purification and characterization of S-linalool synthase, an enzyme involved in the production of floral scent in *Clarkia breweri*. Arch. Biochem. Biophys. **316,** 803–807.

Raguso, R.A., and Pellmyr, O. (1998). Dynamic headspace analysis of floral volatiles: a Comparison of methods. Oikos **81,** 238–254.

Raguso, R.A., and Pichersky, E. (1995). Floral volatiles from *Clarkia breweri* and *C. concinna* (Onagraceae): Recent evolution of floral scent and moth pollination. Plant Syst. Evol. **194,** 55–67.

Trapp, S.C., and Croteau, R.B. (2001). Genomic organization of plant terpene synthases and molecular evolutionary implications. Genetics **158,** 811–832.

Wang, J., Dudareva, N., Bhakta, S., Raguso, R.A., and Pichersky, E. (1997). Floral scent production in *Clarkia breweri* (Onagraceae). II. Localization and developmental modulation of the enzyme *S*-adenosyl-L-methionine:(iso)eugenol *O*-methyltransferase and phenylpropanoid emission. Plant Physiol. **114,** 213–221.

Williams, D.C., McGarvey, D.J., Katahira, E.J., and Croteau, R. (1998). Truncation of limonene synthase preprotein provides a fully active 'pseudomature' form of this monoterpene cyclase and reveals the function of the amino-terminal arginine pair. Biochemistry **37,** 12213–12220.

Wise, M.L., and Croteau, R. (1999). Monoterpene biosynthesis. In Comprehensive Natural Product Chemistry, Vol. 2, Isoprenoids Including Carotenoids and Steroids, D.E. Cane, ed (Oxford, UK: Pergamon Press), pp. 97–153.

(*E*)-β-Ocimene and Myrcene Synthase Genes of Floral Scent Biosynthesis in Snapdragon: Function and Expression of Three Terpene Synthase Genes of a New Terpene Synthase Subfamily

Natalia Dudareva, Diane Martin, Christine M. Kish, Natalia Kolosova, Nina Gorenstein, Jenny Fäldt, Barbara Miller and Jörg Bohlmann

Plant Cell 2003;15;1227-1241; originally published online April 11, 2003;
DOI 10.1105/tpc.011015